

Study of atomic motions in $\text{EuBa}_2\text{Cu}_3\text{O}_{7-\delta}$ using Mössbauer and EXAFS spectroscopies

Short title: atomic motions in $\text{EuBa}_2\text{Cu}_3\text{O}_{7-\delta}$

F. Piazza¹, E. Abraham¹, L. Cianchi², F. Del Giallo², P. Ghigna³, F. Allegretti⁴ and G. Spina⁴

¹ *Heriot-Watt University, Physics Dept - EH14 4AS, Edinburgh, U.K.*

² *IROE, CNR - via Panciatichi 64, 50127 Firenze, Italy*

³ *Università di Pavia, Dip. Chimica Fisica - v.le Taramelli 16, 27100 Pavia, Italy*

⁴ *Università di Firenze, Dip. Fisica - via di S. Marta 3, 50139 Firenze, and INFN*

Pacs 74.72.B

Abstract

We report temperature-dependent Mössbauer and EXAFS measurements of atomic mean square displacements on different samples of $\text{EuBa}_2\text{Cu}_3\text{O}_{7-\delta}$. Our results indicate that the collective atomic motions are characterised by large-amplitude anharmonic oscillations.

1 Introduction

Numerous studies of the vibrational features of superconducting cuprates have shown that some ions in the unit cell of these materials perform large-amplitude anharmonic oscillations even at low temperatures (see *e.g.* [1] and references therein). However, in some cases the results obtained by means of different experimental techniques are not in agreement. For example, both neutron-diffraction [2] and EXAFS experiments [3] reveal vibrational anharmonicity in the motion of apical oxygens. However, neutron diffraction on samples of YBCO single crystals ascribes the anharmonicity to motions in the (a, b) plane, while EXAFS ascribes it to the motion along \hat{c} . Another example: neutron diffraction performed at 10 K on samples of RBCO powders (R= Y and rare earths) [4] showed that the R-ion motion is practically independent of the ion's atomic number, and is consistent with normal atomic vibrations. This result has also been confirmed by neutron diffraction on samples of RBCO single crystals (R=Y,Ho)[2]. However, Mössbauer spectroscopy performed on samples of EuBCO powders measures a much larger mean square displacement (MSD) for the Eu ion [1]. Moreover, the Mössbauer data on samples of EuBCO oriented powders, which will be presented in this paper, also confirm the large low-temperature anharmonicity of the Eu ion, and show that this anharmonicity must be ascribed to the component along \hat{c} . Since there is no plausible reason for the Eu ion to behave differently from Y and the other rare earth ions, we must conclude that Mössbauer data conflict with the neutron ones.

As is well known, the pairing mechanism in high- T_c superconductors is not yet understood. In particular, the role played by the lattice thermal vibrations is still debated (see *e.g.* [5] and references therein). Hence, it is very important to deeply investigate such low-temperature anharmonicities. In order to prove their existence, the MSD must be determined as a function of the temperature. For harmonic crystals, the high temperature trend of the atomic MSD extrapolates through the origin [6]. On the contrary, if the ion moves in a non-parabolic potential, the extrapolation of the high-temperature trend intercepts the y-axis above the origin. The $T = 0$ intercept provides a measure of the “flat” part in the potential-well bottom.

In this article, we present a study of the vibrational features of EuBCO as seen by using both Mössbauer and EXAFS spectroscopies. In particular, Mössbauer spectra of ^{151}Eu in samples of oriented powders will be analysed, in order to investigate the anharmonic components of the motion. On the other hand, EXAFS measurements at the Eu K-edge make it possible to obtain the mean square relative displacements (MSRD) of the Eu ion and

its neighbours. In summary, information on the correlation among atomic motions in the unit cell can be obtained by taking into account Mössbauer and EXAFS data.

2 Mössbauer data

Two samples of oriented single-phase powder (samples 1 and 2) and a sample of randomly-oriented single-phase powder (sample 3) of $\text{EuBa}_2\text{Cu}_3\text{O}_7$ were prepared, all in the form of flat disks. The orientation was obtained by means of two different methods: (1) we mixed the finely-ground powder with epoxy resin, and shaped it in a 8 T magnetic field at room temperature. By doing this, for EuBCO, as for ErBCO, the monocrystalline grains oriented themselves with the \hat{c} axis perpendicular to the magnetic-field [7, 8]. (2) We shaped the powder – a mixture of $\text{EuBa}_2\text{Cu}_3\text{O}_7$ and polyethylene – under a pressure of about 0.3 GPa, thereby orienting the grains with the \hat{c} axis in the direction of the pressure. Finally, we obtained sample 3 simply by mixing the powder with epoxy resin. The orientation degree was determined by means of X-ray Bragg diffraction with Bragg-Brentano acquisition geometry. The orientation distribution is Gaussian in the cosine of the orientation angle for both samples, with standard deviations of 15° for the magnetically oriented sample and about twice as much for the one oriented under pressure. The transition temperature for all the samples is 92 K.

We collected six spectra at the temperatures $T=20, 85, 90, 95, 200$ and 300 K for each sample, using a standard spectrometer with a SmF_3 source of 3.7 GBq at room temperature. From the analysis of the spectra, we calculated the ratio between the Debye-Waller factors in the \hat{c} and (\hat{a}, \hat{b}) directions as functions of the temperature. We carried out this analysis for the two oriented samples, combining them with the results from the isotropic sample. We got the same value for the ratio f_c/f_{ab} in the two cases, thereby obtaining a good cross-check for the reliability of the measurement. This also provided direct evidence of consistency of data sets from the different grain-aligned samples. A detailed description of this analysis will be given elsewhere¹. The $f_c/f_{a,b}$ ratio turned out about 0.4 at all temperatures. This means that the motion of the Eu ion is anisotropic, the amplitude in \hat{c} direction being greater than the one in the (\hat{a}, \hat{b}) plane. By combining this result with the previous Mössbauer measurements of the angular-averaged ^{151}Eu MSD [1], we can calculate $\langle x_c^2 \rangle$ and $\langle x_{ab}^2 \rangle$. The results of these calculations are plotted in fig. 1. We note that the MSD of the \hat{c} -component is

¹work in preparation

about three times greater than the (\hat{a}, \hat{b}) -component. Moreover, the $T = 0$ intercept of the high temperature trends of both components do not cross the origin. Consequently, our Mössbauer data show low-temperature anharmonicities, both along \hat{c} and in the (\hat{a}, \hat{b}) plane.

3 EXAFS data

We prepared two samples of $\text{EuBa}_2\text{Cu}_3\text{O}_{7-\delta}$ single-phase powders mixed with polyethylene, with $\delta \approx 1$ (nonsuperconducting) and $\delta \approx 0$ ($T_c \approx 90$ K). For each of them, we collected transmission Eu K-edge EXAFS spectra at $T = 30, 60, 90, 120, 180, 250$ and 300 K. The measurements were performed at the beam-line GILDA CRG of the European Synchrotron Radiation Facility (ESRF) in Grenoble.

The model cluster used for the EXAFS calculations is shown in fig. 2, which represents the local structure around Eu in EuBCO up to a radial distance of 4 \AA . The four shells included in the calculations are denoted as Eu-O, Eu-Cu, Eu-Ba and Eu-Eu(2), in order of (their) increasing distance from Eu. Actually, the EXAFS Fourier transform shows further components above 4 \AA , but their analysis is much less accurate. Therefore, they have not been considered in fitting the experimental data. A typical EXAFS signal with corresponding Fourier Transform is shown in fig. 3.

We carried out the data analysis by fitting the experimental spectra with the aid of the GNXAS package [9], with distances R_i and Debye-Waller factors σ_i^2 as fitting parameters, beside the energy threshold E_0 used in the energy-to-wavevector conversion. We found that the average distances between europium and its neighbours do not vary appreciably (less than 0.5% for temperatures up to 300 K). The trends of the MSD's are more interesting. The best fit results are reported in table 1 and table 2 for the samples with $\delta \approx 0$ and $\delta \approx 1$, respectively. It can be seen that they lie in a range which is consistent with normal harmonic vibration (see *e.g.* [10], where the σ^2 values for copper are reported). Moreover, the σ^2 's of the first two shells do not depend on the doping. On the contrary, the σ_i^2 's corresponding to the Ba and Eu(2) shells are observed to be somewhat smaller for the overdoped sample.

4 Correlations among ionic motions

As is well known, the EXAFS Debye-Waller factors measure the broadening of the bond distances due to the thermal motions, provided the static

disorder is negligible. Then, denoting by σ_1^2 and σ_2^2 the absorber and the backscatterer MSD's along the interatomic distance R_{12} respectively, the corresponding σ_{EXAFS}^2 is given by:

$$\sigma_{EXAFS}^2 = \sigma_1^2 + \sigma_2^2 - 2\rho_{12}\sigma_1\sigma_2 \quad (1)$$

where ρ_{12} denotes the so-called correlation parameter. If $\rho_{12} \approx \pm 1$, the motion is highly correlated, in-phase or out-of-phase, respectively. If $\rho_{12} \approx 0$, the ionic oscillations are uncorrelated. Generally, a decrease of $|\rho_{12}|$ is expected as the interatomic distance increases. Furthermore, if the Debye model is a good approximation for the considered solid, ρ_{12} is expected to be an increasing function of temperature. This is a consequence of the correlations, as seen by EXAFS, being projected onto the absorber-backscatterer bond distance, thereby being 1D correlations in their very nature [11].

Some qualitative conclusions regarding the correlations among ion motions are drawn here as follows. Let us consider the ionic radii of Eu^{3+} and O^{2-} . We see that the two ions are practically in contact with each other [12]. Consequently, a large positive correlation between the motions of the europium and the oxygen ions of the first shell is expected. Moreover, taking into account the tight binding between the oxygen and copper ions in the CuO_2 planes, a large positive correlation is also expected with the copper ions of the second shell [13]. On the other hand, we note that Ba^{2+} ions are not in contact with the inner shells. Nevertheless, the corresponding measured σ^2 show to be rather small. Then, in order for these results to be consistent with the large oscillation of the Eu ion along \hat{c} as measured by Mössbauer spectroscopy, a large positive correlation between the two ions has to exist. Finally, we can combine the Mössbauer value for the σ_{Eu}^2 in the (\hat{a}, \hat{b}) plane with the σ_{EXAFS}^2 to calculate $\rho_{\text{Eu-Eu}}$ as a function of temperature. Unlike the normal trend, $\rho_{\text{Eu-Eu}}$ decreases monotonically from ≈ 1 to ≈ 0.75 as the temperature increases from 30 to 300 K.

5 Conclusions

By combining the Mössbauer and EXAFS results with the expected scenario of a large positive correlation between the motions of Eu and O ions, we suggest that the ionic motions consist of large-amplitude, highly-correlated oscillations with superimposed small-amplitude, weakly-correlated, vibrations. The large-amplitude component can be described as follows. Starting from the equilibrium configuration, let us imagine we displace the Eu ion along \hat{c} . As a consequence, the oxygen ions will move along the line joining

the Eu and O centres, see fig. 4. But this displacement hardly changes the Eu–O distance and therefore, it will not be revealed by EXAFS. Hence, the measured $\sigma_{\text{Eu-O}}^2$'s correspond only to the small-amplitude component. The same considerations apply to the Cu ions, since their motions are closely correlated with the motions of the oxygen neighbours [13].

The rather small values of $\sigma_{\text{Eu-Ba}}^2$ measured in our experiment may seem surprising. In fact, since Ba^{+2} ions are not in contact with the inner shells, the large-amplitude oscillations of Eu along \hat{c} , as measured by Mössbauer spectroscopy, would result in a large-amplitude relative motion for these two ions. However, $\sigma_{\text{Eu-Ba}}^2$'s are fairly small. Consequently, we should conclude that the motions of barium and europium are strongly and positively correlated, despite their rather large separation. A possible explanation could be that, due to coulomb interaction between the Eu^{+3} and Ba^{+2} ions, when the former moves in a certain direction the latter is forced to move in the same direction, and *viceversa*. We also note that the large displacements of the oxygen ions result in a variation of the sum of their attractive forces on the barium ions. This, in turn, increases the correlation between europium and barium motions. To summarise, the large anharmonic oscillation includes the Eu and Ba motions along \hat{c} and the rotation around the cell centre of the oxygen ions of the first shell.

Finally, we observe that our experiments do not reveal remarkable differences between the underdoped and overdoped samples. The $\sigma_{\text{Eu-O}}^2$ and $\sigma_{\text{Eu-Cu}}^2$ values clearly show that the relative motions of these ions are independent of the doping level. On the contrary, the $\sigma_{\text{Eu-Ba}}^2$ and $\sigma_{\text{Eu-Eu}}^2$ values of the overdoped sample are significantly smaller than those of the underdoped one at $T < T_c$. Such a difference could be due to the coupling phenomenon that takes place at $T < T_c$ in the superconducting sample. However, in order to clarify this question, further investigations will be necessary. We also note that the observed decrease in $\rho_{\text{Eu-Eu}}$ as the temperature increases cannot be explained within the framework of phonon theory.

References

- [1] Capaccioli M., Cianchi L., Del Giallo F., Pieralli F., and Spina G. 1995 *J. Phys. Cond. Matter* **7** 2429.
- [2] Schweiss P., Reichardt W., Braden M., Collin G., Heger G., Claus H. and Erb A. 1994 *Phys. Rev. B* **49** 1387
- [3] Mustre de Leon J., Conradson S. D., Batistić I., and Bishop A. R. 1990 *Phys. Rev. Lett.* **65** 1675
- [4] Guillaume M., Allenspach P., Mesot J., Roessli B., Staub U., Fischer P. and Furrer A. 1993 *Z. Phys. B* **90** 13
- [5] J. F. Annett, N. Goldenfeld and A. J. Leggett 1996 *Physical Properties of High Temperatures Superconductors* Ed D. M. Ginsberg Vol (5) World Scientific
- [6] Kolk B. *Dynamical Properties of Solids* Ed G. K. Horton and A. A. Maradudin 1984 Vol(5) Elsevier NY 1
- [7] knorr D. B. and Livingston J. D. 1989 *Supercon. Sci. Technol.* **1** 302
- [8] Durand L., Kircher F., Régnier P., Chateigner D., Pellerin N., Gotor F. J., Simon P. and Odier P. 1995 *Supercon. Sci. Technol.* **8** 214
- [9] Filippini A. and Di Cicco A. 1996 <http://camcnr.unicam.it/www/gnxas.html>
- [10] Greigor R. B. and Lytle F. W. 1979 *Phys.Rev. B* **20** 4902
- [11] Beni G. and Platzman P. M. 1976 *Phys.Rev. B* **14** 1514
- [12] Values of 1.4 Å and 1.08 Å are reported at <http://www.webelements.com> for the O²⁻ and Eu³⁺ ions respectively. They add up to 2.48 Å, when the Eu–O bond distance is 2.41 Å from our measurements and in good agreement with crystallographic data.
- [13] Lanzara A., Saini N. L., Bianconi A., Duc F. and Bordet P. 1999 *Phys. Rev. B* **59** 3851

Figures and Tables

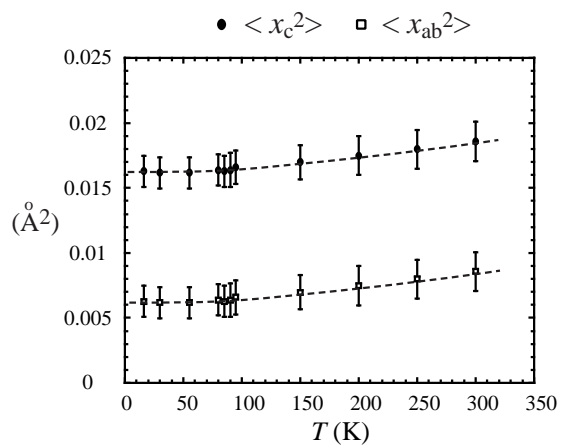


Figure 1: Trend of the MSD along \hat{c} and in the \hat{ab} planes as a function of the temperature

s

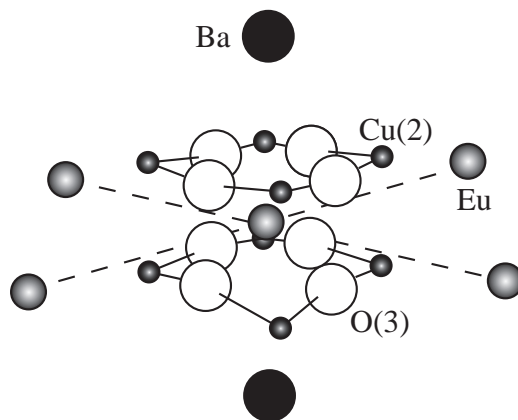


Figure 2: Cluster used in the simulation of the EXAFS spectra. In order of increasing distance from the Eu site, one can see the O shell, the Cu shell, the Ba shell and the shell of Eu's lying in the adjacent cells.

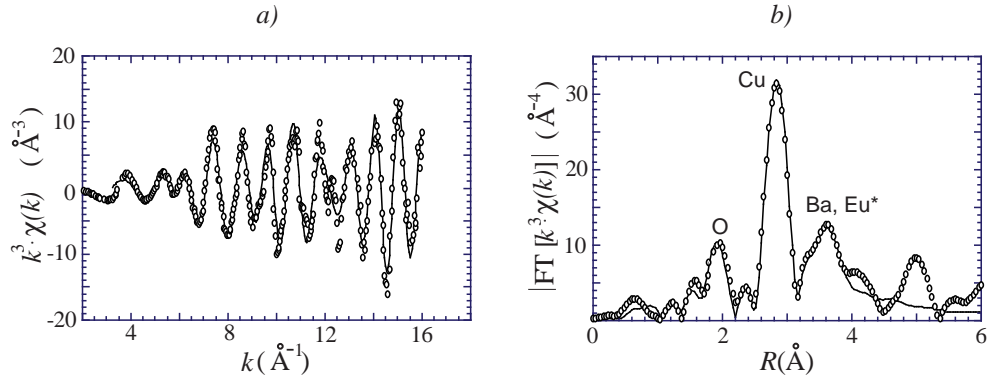


Figure 3: *a)* Eu K-edge EXAFS signal measured in the underdoped sample at a representative temperature $T = 30$ K multiplied by k^3 . Circles are experimental points. The solid line is the result of the fit. *b)* Magnitude of the Fourier transform of the representative signal shown beside. Small circles: experimental. Solid line: fit. The fit of the signal for $k \approx 12 \text{\AA}^{-1}$ is less accurate. This is because the contribution to the spectra for $k \approx 12$ comes from the remote shells, which are not taken into account in our signal calculation.

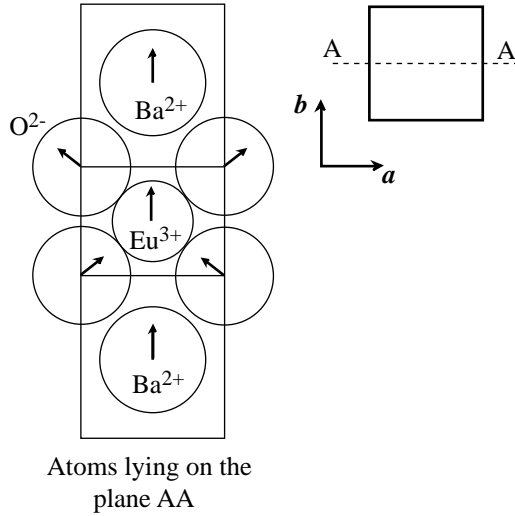


Figure 4: Schematic representation of the O and Ba shells in an EBCO unit cell drawn to scale. The arrows represent large displacements of the ions, which are caused by a large displacement of the europium ion along \hat{c} .

Table 1: EXAFS-MSRD's for the underdoped EBCO.

T (K)	σ_{O}^2 (10^{-3}\AA^2)	σ_{Cu}^2 (10^{-3}\AA^2)	σ_{Ba}^2 (10^{-3}\AA^2)	σ_{Eu}^2 (10^{-3}\AA^2)
30	4.0(5)	2.1(2)	3.0(6)	2.2(3)
60	4.1(5)	2.2(2)	3.5(7)	2.2(3)
90	4.4(5)	2.5(2)	3.9(8)	2.4(3)
120	4.7(6)	2.9(2)	4.1(9)	3.2(4)
180	5.5(7)	3.7(3)	4.6(10)	4.2(5)
250	6.7(9)	4.7(3)	5.5(16)	5.1(8)
300	8.1(11)	5.2(4)	7.4(19)	6.0(10)

Table 2: EXAFS-MSRD's for the overdoped EBCO.

T (K)	σ_{O}^2 (10^{-3}\AA^2)	σ_{Cu}^2 (10^{-3}\AA^2)	σ_{Ba}^2 (10^{-3}\AA^2)	σ_{Eu}^2 (10^{-3}\AA^2)
30	4.2(7)	2.0(2)	1.4(4)	1.3(3)
60	4.2(7)	2.0(2)	1.4(4)	1.3(3)
90	4.4(8)	2.5(2)	2.4(6)	1.6(3)
120	4.7(8)	2.8(2)	2.7(7)	2.3(8)
180	5.3(10)	3.4(3)	2.8(9)	3.2(12)
250	6.8(12)	4.8(3)	4.4(14)	5.3(18)
300	7.5(12)	5.2(4)	4.8(12)	5.7(16)